

# Study of Possible Local Quasars IV. Effects of Discretization in Relations for QSOs and Search for Quasar-Stellar-Planetary Connections

Kiril P. Panov\*

*Institute of Astronomy and National Astronomical Observatory, Bulgarian Academy of Sciences, Sofia, Bulgaria*

**Abstract:** Relations for possible local quasars are studied: the “mass-radius”, “density-mass”, and “radius-density” relations. These relations show clear fragmentation and which is due to the presence of parallel sequences of observations. The cause for this unusual fragmentation is the presence of a term depending on  $r_{gr}/r_q$  in each respective relation. It seems therefore that fragmentation in these relations is due to evolution of quasars: as QSOs evolve, the ratio  $r_{gr}/r_q$  takes a sequence of discrete values and for each of these values there is a corresponding (different) relation. Each one of these three relations: “mass-radius”, “density-mass”, and “radius-density” evolve with the evolution of  $r_{gr}/r_q$ , building a “family” of relations.

It is shown that the “mass-radius”, “density-mass”, and “radius-density” relations in their present versions hold also for stars, planets, and satellites, as well as for quasars. The linear density relation found previously for quasars and stars is now shown to apply also to the 9 planets and 19 satellites of the solar system. The existence of common relations, identical for quasars, stars, and planets leads to the conclusion that a link should probably exist between these structures. This link could be hidden in the origin of all these structures. The controversy with the gravitational collapse theory is obvious and needs further study.

**Keywords:** Evolution of quasars, origin of quasars, relations for quasars, stars and planets.

## 1. INTRODUCTION

Studies of possible local quasars were recently carried out in [1-3]. The results of these studies seem to be consistent with the following concepts:

- Local quasars exist around some low redshift galaxies, possibly being ejected by the active galactic nuclei of these (parent) galaxies [4-29, and references therein].

- The observed quasar redshifts are composed of three components: cosmological redshift, gravitational (intrinsic) reddening, and Doppler shift [30].

- Local quasars evolve with increasing radii and luminosities, and with decreasing densities and redshifts [1-3].

- The cause of quasar evolution, as well as the cause of several relations, found for local quasars could be disintegration of some primordial, dense matter, suggested by Ambarsumian [31].

- Local quasars evolve into small mass, companion galaxies [32, 33].

Relations for possible local quasars were found in [1-3]. Some of these relations seem to be unusually fragmented: the “mass-radius”, the “density-mass”, and the “radius-density” relations [3]. The unusually fragmented shapes of

these diagrams (see Figs. 1-3) are due to the presence of parallel sequences of observations, apparently having the same slope. Apparently, some of these parallel sequences are more densely “populated” with QSOs than others. This strange appearance does not look as being caused by random errors and it may even cast doubt on the procedure used in [1-3].

Could the peculiar fragmentation mentioned above be due to the evolution of quasars? To answer this question, some theoretical treatment is necessary.

In [3], a linear density relation was obtained and applied to quasars and stars. It would be interesting to study if the same relation could hold also for planets and satellites.

## 2. THE “MASS-RADIUS” RELATION

From Eq. (10) of [3], we have for the quasars’ density:

$$\rho_q = 3/(8\pi) \cdot c^2/G \cdot 1/r_q^2 \cdot (r_{gr}/r_q) \quad (1)$$

here  $r_{gr}$  and  $r_q$  are the gravitational radius and the quasar radius, and  $G$  and  $c$  are the gravitational constant and the velocity of light, respectively. With simple transformations we get for the mass-radius ratio:

$$m_q/r_q = c^2/(2G) \cdot (r_{gr}/r_q) \quad (2)$$

Further we get (in the cm, g, s-system):

$$\log m_q = 27.83 + \log r_q + \log (r_{gr}/r_q) \quad (3)$$

Eq. (3) is the “mass-radius” relation, found in [1] and confirmed in [2-3]. However, from Eq. (3) it is apparent that an additional term is present, depending on  $r_{gr}/r_q$ .

\*Address correspondence to this author at the Institute of Astronomy and National Astronomical Observatory, Bulgarian Academy of Sciences, Sofia, Bulgaria; Tel: 029741910; Fax: 029741910; E-mail: [kiril\\_panov@yahoo.com](mailto:kiril_panov@yahoo.com)

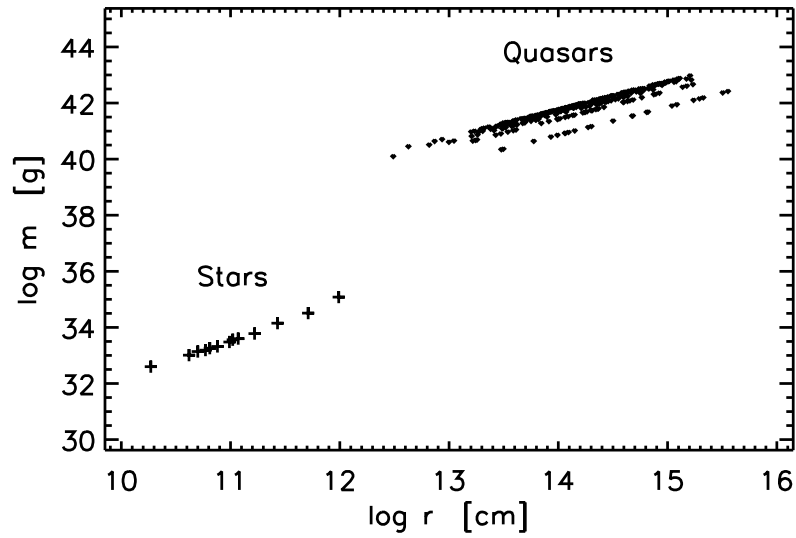


**Fig. (1).** The relation “mass-radius” for 341 sample quasars (dots). The lowest sequence of QSOs corresponds to  $r_{gr}/r_q = 0.11$ . The same relation is shown also for stars (crosses), as mean values for O5, B0, B5, ..., M5.

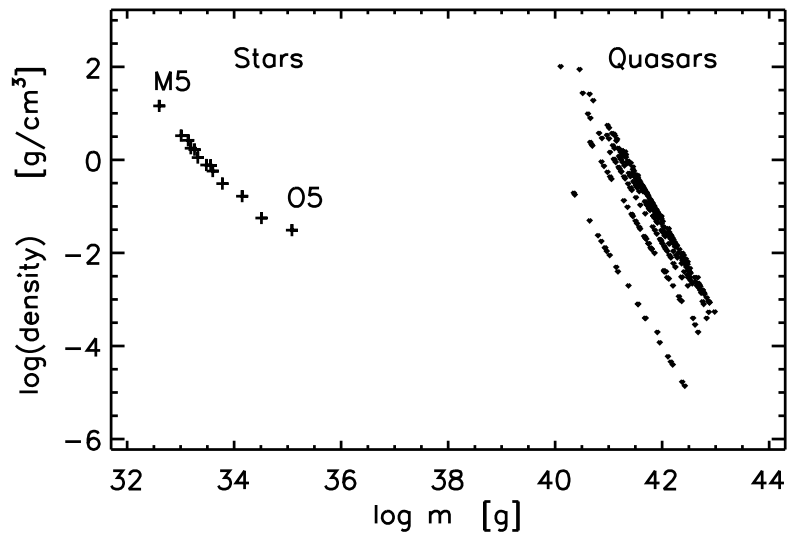


**Fig. (2).** Relation “density-mass” for the sample of 341 quasars (dots). The lowest sequence corresponds to  $r_{gr}/r_q = 0.11$ . The same relation is shown for stars (crosses), as mean values for O5, B0, B5, ..., M5.

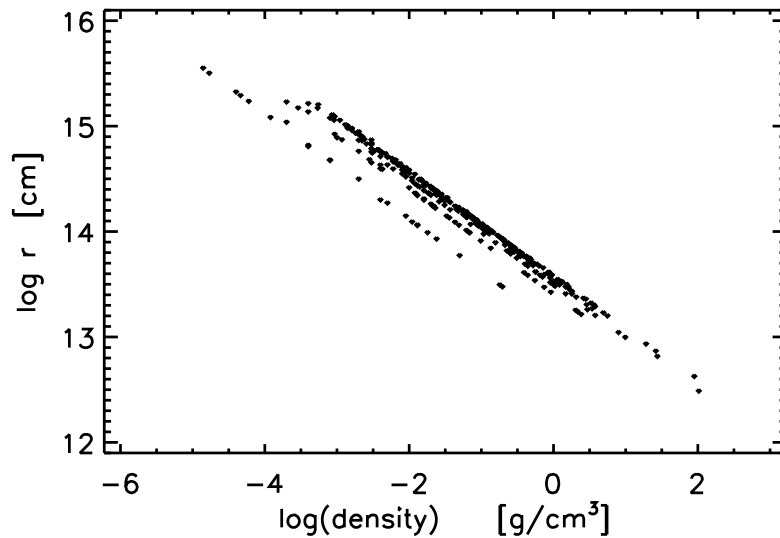


**Fig. (3).** Relation “radius-density” for 341 sample quasars. The lowest sequence corresponds to  $r_{gr}/r_q = 0.11$ .

**Table 1. Fitting coeff for Eqs. (4) for the sample of 341 QSOs [2-3], divided in groups according to respective  $r_{gr}/r_q$ .**

Number QSOs	$r_{gr}/r_q$	$z_{gr}$	Coefficients from Eqs. (4)		Coefficients from Observations		Corr. coeff
			a	b	a	b	
23	0.11	0.06	26.87	1.0	26.87	0.999	0.999
40	0.41	0.30	27.44	1.0	27.44	1.0	1.0
41	0.61	0.60	27.62	1.0	27.62	0.999	1.0
57	0.74	0.96	27.70	1.0	27.70	1.0	1.0
61	0.83	1.41	27.75	1.0	27.75	1.0	1.0
103	0.89	1.96	27.78	1.0	27.81	0.997	1.0
15	0.92	2.64	27.79	1.0	27.80	1.0	1.0

As shown in [1-3],  $r_{gr}/r_q$  take discrete values: 0.11, 0.41, 0.61, 0.74, 0.83, 0.89, 0.92, and so on. These values correspond respectively to gravitational redshifts: 0.06, 0.30, 0.60, 0.96, 1.41, 1.96, 2.64, and so on. Therefore, with substitution of respective  $r_{gr}/r_q$  value, we get from Eq. (3) a whole family of relations:

$$\begin{aligned}
 &\text{for } r_{gr}/r_q = 0.11, \log m_q = 26.87 + \log r_q \\
 &\text{for } r_{gr}/r_q = 0.41, \log m_q = 27.44 + \log r_q \quad (4) \\
 &\dots\dots\dots \\
 &\text{for } r_{gr}/r_q = 0.92, \log m_q = 27.79 + \log r_q \\
 &\dots\dots\dots \\
 &\text{for } r_{gr}/r_q = 1.0, \log m_q = 27.83 + \log r_q
 \end{aligned}$$

The family of Eqs. (4) defines a family of parallel lines with a slope of 1, and which are indeed seen in Fig. (1). The lowest line corresponds to  $r_{gr}/r_q = 0.11$ , and in direction of increasing values of  $r_{gr}/r_q$  the parallel lines get closer and “converge” to a limit, corresponding to  $r_{gr}/r_q = 1.0$ . With decreasing distance between successive lines they actually become undistinguishable for high values of  $r_{gr}/r_q$  due to observational uncertainties. In order to test Eqs. (4) with the observations of QSOs, the sample of 341 QSOs [2-3] was divided in groups, each group having the same  $r_{gr}/r_q$ . For each group the coefficients of the linear equations were evaluated which are listed in Table 1 (columns are self-explanatory). Comparison of the coefficients of Eqs. (4) with the fit of observations is shown in columns 4 and 5 of Table 1, and the agreement is obvious.

Using the same sample of 341 QSOs, the average relation was established [3]:

$$\log m_q = 28.67 + 0.93 \log r_q \quad (5)$$

The differences in the coefficients between Eq. (5) and Eqs. (4) are obviously due to the unequal “population” of the different parallel lines with observations. This is shown with the number of QSOs in the first column of Table 1. If an average relation is built over the whole sample, the result will be slightly different from the coefficients in Eqs. (4).

The question of limit of convergence in Eqs. (4) should also be addressed. From [3], we have:

$$r_{gr}/r_q = 1 - 1/(1 + z_{gr})^2 \quad (6)$$

Therefore, if  $z_{gr} = \infty$ ,  $r_{gr}/r_q = 1$ . It should be noted that this limit for  $r_{gr}/r_q$  holds for any choice of the radius of reduction of quasars’ densities, not only for the specific radius  $r = 8 \cdot 10^{13}$  cm, chosen in [1-3]. It looks therefore that as quasars evolve so does also the ratio  $r_{gr}/r_q$ , starting (theoretically) with 1, and going down with increasing steps to 0.11 (last). Correspondingly, the “mass-radius” relation moves from the limit of convergence ( $r_{gr}/r_q = 1$ ) to the lowest line ( $r_{gr}/r_q = 0.11$ ) in Fig. (1). This transition (evolution) of the “mass-radius” relation is however not continuous but proceeds in steps, according to the sequence of  $r_{gr}/r_q$ . The agreement of theory and observations (Table 1) is satisfactory. Looking into details of Fig. (1), the transition of the “mass-radius” relation seems to proceed with increasing radius, but with decreasing mass.

### 3. THE “DENSITY-MASS” RELATION

In Fig. (2), the observational diagram “density-mass” is shown for the sample of 341 QSOs [2-3]. Again, this diagram is fragmented and parallel sequences are seen. One could start again with the Eq. (2):

$$m_q/r_q = c^2/(2G) \cdot (r_{gr}/r_q)$$

With simple transformations we get:

$$\rho_q = 3/(32\pi) \cdot (c^6/G^3) \cdot (1/m_q^2) \cdot (r_{gr}/r_q) \quad (7)$$

and further:

$$\log \rho_q = 82.86 - 2 \cdot \log m_q + 3 \cdot \log (r_{gr}/r_q) \quad (8)$$

Eq. (8) is the “density-mass” relation from [1-3] and defines a family of relations, corresponding to the sequence of  $r_{gr}/r_q$ :

$$\begin{aligned}
 &\text{for } r_{gr}/r_q = 0.11, \log \rho_q = 79.98 - 2 \cdot \log m_q \\
 &\text{for } r_{gr}/r_q = 0.41, \log \rho_q = 81.70 - 2 \cdot \log m_q \quad (9) \\
 &\dots\dots\dots \\
 &\text{for } r_{gr}/r_q = 0.92, \log \rho_q = 82.75 - 2 \cdot \log m_q \\
 &\dots\dots\dots \\
 &\text{for } r_{gr}/r_q = 1.0, \log \rho_q = 82.86 - 2 \cdot \log m_q
 \end{aligned}$$

**Table 2. Fitting coeff for Eqs. (9) for the sample of 341 QSOs [2-3], divided in groups according to respective  $r_{gr}/r_q$ .**

Number QSOs	$r_{gr}/r_q$	$z_{gr}$	Coefficients from Eqs. (9)		Coefficients from observations		Corr. coeff
			a	b	a	b	
23	0.11	0.06	79.98	-2.0	79.21	-1.98	-0.999
40	0.41	0.30	81.70	-2.0	81.71	-2.0	-1.0
41	0.61	0.60	82.22	-2.0	81.98	-2.0	-1.0
57	0.74	0.96	82.47	-2.0	82.28	-2.0	-1.0
61	0.83	1.41	82.62	-2.0	82.63	-2.0	-1.0
103	0.89	1.96	82.71	-2.0	82.94	-2.0	-1.0
15	0.92	2.64	82.75	-2.0	82.42	-1.99	-1.0

**Table 3. Fitting coeff for Eqs. (11) for the sample of 341 QSOs [2-3], divided in groups according to respective  $r_{gr}/r_q$ .**

Number QSOs	$r_{gr}/r_q$	$z_{gr}$	Coefficients from eqs (11)		Coefficients from observations		Corr. coeff
			a	b	a	b	
23	0.11	0.06	13.12	-0.50	13.12	-0.50	-1.0
40	0.41	0.30	13.41	-0.50	13.41	-0.50	-1.0
41	0.61	0.60	13.49	-0.50	13.495	-0.50	-1.0
57	0.74	0.96	13.53	-0.50	13.54	-0.50	-1.0
61	0.83	1.41	13.56	-0.50	13.56	-0.50	-1.0
103	0.89	1.96	13.57	-0.50	13.578	-0.50	-1.0
15	0.92	2.64	13.58	-0.50	13.586	-0.50	-1.0

The family Eqs. (9) represents a family of parallel lines with a slope of -2, and these lines get closer in direction of increasing  $r_{gr}/r_q$ , becoming eventually undistinguishable from each other (because of observational uncertainties). From Fig. (2), the same picture is apparent. The limiting value for  $r_{gr}/r_q$  is 1.

In [1] and [2], an average equation “density-mass” has been determined with slightly different coefficients. Both of these relations deviate also from Eqs. (9). The cause for that is partly in the different samples of QSOs in [1] and [2], and partly in the distribution of observations over  $r_{gr}/r_q$ , as explained above. Using the sample of 341 QSOs [2-3], Eqs. (9) are fitted to the groups of QSOs with respective  $r_{gr}/r_q$ . The results are shown in Table 2.

Comparison of observations with the theoretical values from Eqs. (9) shows satisfactory agreement. The same remark (as in the previous section) is due also for the “density-mass” relation: presumably, with the evolution of quasars evolves also  $r_{gr}/r_q$ , and the respective “density-mass” relation. The last lower line corresponds to  $r_{gr}/r_q = 0.11$ . Looking into details of Fig. (2), the transition of the “density-mass” relation seems to proceed with decreasing density, and possibly also with a decreasing mass.

**4. THE “RADIUS-DENSITY” RELATION**

The “radius-density” relation for quasars was established in [3]. In Fig. (3), the relation is presented for the sample of

341 QSOs [2-3] and the fragmentation (parallel sequences of observations) is clearly seen. For a theoretical background, we could start again with the Eq. (1):

$$\rho_q = 3/(8\pi) \cdot c^2/G \cdot 1/r_q^2 \cdot (r_{gr}/r_q)$$

With simple transformations we get:

$$\log r_q = 13.60 - \frac{1}{2} \log \rho_q + \frac{1}{2} \log (r_{gr}/r_q) \tag{10}$$

This is the “radius-density” relation found in [3]. With the sequence of  $r_{gr}/r_q$  values, Eq. (10) represents a family of relations:

$$\begin{aligned} &\text{for } r_{gr}/r_q = 0.11, \log r_q = 13.12 - \frac{1}{2} \log \rho_q \\ &\text{for } r_{gr}/r_q = 0.41, \log r_q = 13.41 - \frac{1}{2} \log \rho_q \\ &\dots\dots\dots \\ &\text{for } r_{gr}/r_q = 0.92, \log r_q = 13.58 - \frac{1}{2} \log \rho_q \\ &\dots\dots\dots \\ &\text{for } r_{gr}/r_q = 1.0, \log r_q = 13.60 - \frac{1}{2} \log \rho_q \end{aligned} \tag{11}$$

The sample of 341 QSOs [2-3] was divided again in groups, according to respective  $r_{gr}/r_q$ , and the Eqs. (11) were fitted to observations. The results are shown in Table 3. The comparison of theoretical and the fitting coefficients (columns 4 and 5) show satisfactory agreement. Again, the family of parallel relations (11) converges to a limit, corresponding to  $r_{gr}/r_q = 1$ . Presumably, as quasars evolve, so evolves

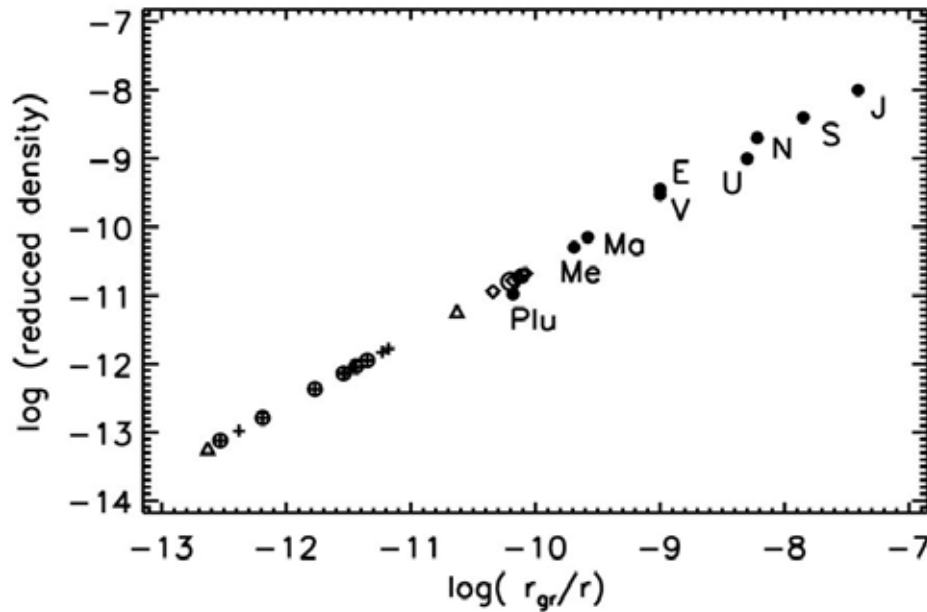


**Fig. (4).** Reduced density [g/cm<sup>3</sup>] to  $r = 8.10^{13}$ cm, versus  $r_{gr}/r$  for planets and satellites of the solar system. Dots – planets, empty circle – the Moon, rhombs – satellites of Jupiter (Io, Europa, Ganymede, Callisto), crossed circles – satellites of Saturn (Mimas, Enceladus, Thetis, Dione, Rhea, Titan, Iapetus), crosses – satellites of Uranus (Ariel, Umbriel, Titania, Oberon, Miranda), and triangles – satellites of Neptune (Triton and Nereid). At the left lower end is Nereid.

**Table 4.** Fitting coefficients of Eq. (12) for 341 quasars [2-3], for stars of spectral classes B0, B5, A0,....., M5 (mean values), for 9 big planets of the solar system, and for 19 satellites (Moon, Io, Europa, Ganymede, Callisto, Mimas, Enceladus, Thetis, Dione, Rhea, Titan, Iapetus, Ariel, Umbriel, Titania, Oberon, Miranda, Triton, Nereid).

	Coeff "a"	Coeff "b"	Correlation coeff	Range of the reduced density [g/cm <sup>3</sup> ] to $8.10^{13}$ cm
341 quasars	0.0002	0.251	0.998	0.02 - 0.25
Stars B0-M5	$-2.10^{-9}$	0.2505	0.998	$0.8.10^{-6}$ - $2.3.10^{-6}$
9 Planets	$7.10^{-11}$	0.258	0.998	$1.1.10^{-11}$ - $1.10^{-8}$
19 Satellites	$-2.10^{-16}$	0.25155	0.9999	$5.9.10^{-14}$ - $2.1.10^{-11}$

also  $r_{gr}/r_q$ , and the “radius-density” relation evolves also stepwise, starting with  $r_{gr}/r_q = 1$ . The last lower sequence corresponds to  $r_{gr}/r_q = 0.11$ . Looking into details of Fig. (3), it seems that the transition (evolution) of the “radius-density” relation proceeds with increasing radius and decreasing density, in agreement with the concept of disintegration.

### 5. THE LINEAR DENSITY RELATION FOR PLANETS AND SATELLITES

In [3] it was shown that a linear density equation exists and which could be applied to both quasars and stars:

$$\rho \tilde{=} 0.251549. (r_{gr}/r) \tag{12}$$

with  $\rho \tilde{}$  being the reduced densities to a radius of  $8.10^{13}$  cm,  $r_{gr}$  and  $r$  being the gravitational radius and the actual radius of respective object. The same equation seems to hold also for the 9 big planets of the solar system. We could try to apply relation (12) to 19 big satellites of the solar system. In Fig. (4), a cumulative diagram is shown for planets and satellites on a logarithmic scale. The applicability of the linear density Eq. (12) is obvious.

Note that transition from planets to satellites is smooth, while there are jumps by the transition “quasars-to-stars”, and “stars-to-planets”. In Table 4, data for fitting coefficients of Eq. (12) are listed for quasars, stars, planets, and satellites.

The applicability of the linear density Eq. (12) to such different structures as quasars, stars, planets, and satellites is really surprising and could have far reaching consequences for theories of their origin. It seems possible that a link between these structures could exist in their origin. The discussion of possible links will follow. Although this matter is as yet far from clear, it could present severe difficulties for the theory of gravitational collapse. Next I will turn to the previously studied relations, “mass-radius”, “density-mass”, and “radius-density”, and try to apply these relations to stars, planets, and satellites.

### 6. CUMULATIVE DIAGRAMS FOR QSOs, STARS, AND PLANETS

The relations (3, 8, and 10) were obtained considering very general physical relations, which are expected to hold not only for quasars but also for stars and planets. Therefore,

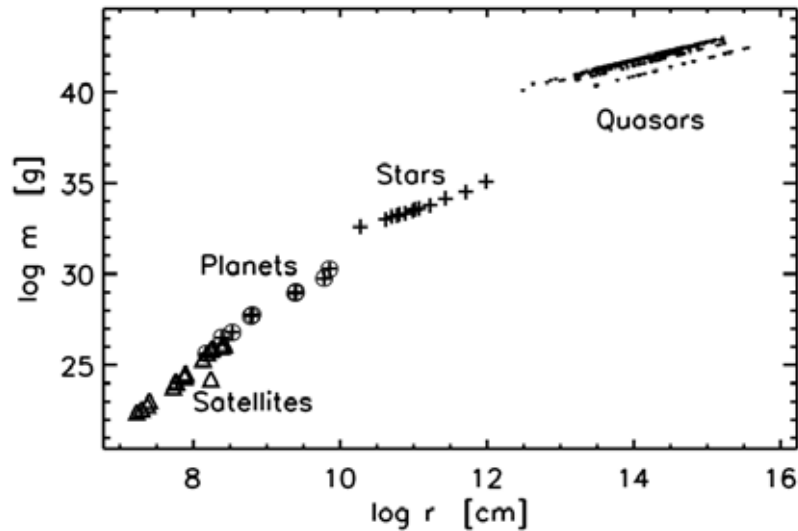


**Fig. (5).** Cumulative diagram of the “mass-radius” relation for quasars (dots), stars O5, B0, B5,...M5 (crosses), for 9 big planets of the solar system (encircled crosses), and for 19 satellites (triangles, the list is as in caption of Table 4).

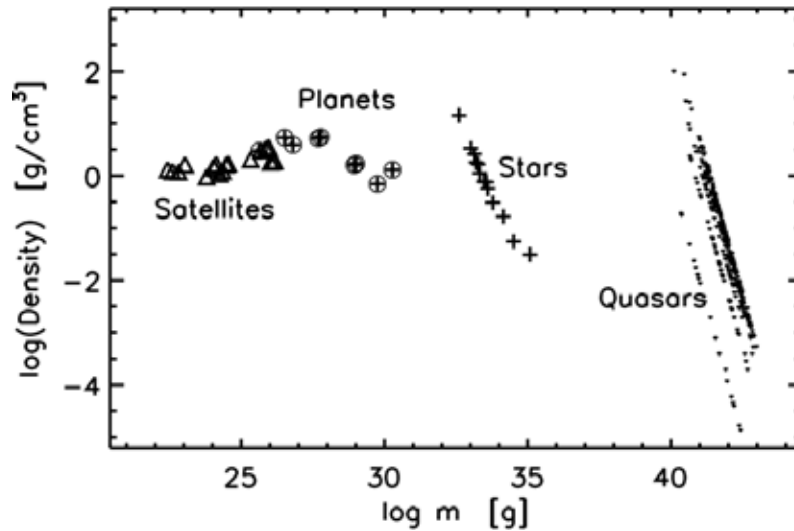


**Fig. (6).** Cumulative diagram of the “density-mass” relation for quasars (dots), stars (crosses), the 9 big planets of the solar system (encircled crosses), and for 19 satellites (triangles, the list is as in caption of Table 4).

relations (3, 8, and 10) could also be expected to hold for stars and planets. Indeed, for the verification of the above assumption, the relations (3, 8, and 10) will be written again without subscripts “q” as:

$$\log m = 27.83 + \log r + \log (r_{gr}/r) \tag{13}$$

$$\log \rho = 82.86 - 2.\log m + 3.\log (r_{gr}/r) \tag{14}$$

$$\log r = 13.60 - \frac{1}{2} \log \rho + \frac{1}{2} \log (r_{gr}/r) \tag{15}$$

In relations (13-15), the masses, radii, gravitational radii, and densities are considered separately for stars, or for planets, or for satellites, respectively. In the right side of these equations the observational values are put and the left sides (masses  $m$ , densities  $\rho$ , and radii  $r$ ) are calculated. Then these calculated values are compared with the respective observational values. The comparison is shown in Table 5.

The agreement of observed and calculated values is satisfactory, showing that Eqs. (13-15) hold also for stars, planets, and satellites, as well as for quasars. The discrepancies

between observed and calculated values are generally a few percent. Only for O- stars and for the planet Pluto discrepancies are quite large. Two factors could contribute to these discrepancies. Relations (13-15) do not take into account possible oblateness, i.e. they hold only for spherical bodies. The second factor is observational uncertainties.

In Fig. (5), a diagram “mass-radius” is shown for quasars, stars, planets, and satellites of the solar system. Two remarks are due to this diagram. The slopes are gradually increasing from QSOs to satellites. The second remark concerns the jumps between different structures. The jump from QSOs to stars is quite large, in both masses and radii. The jump from stars to planets gets smaller, and there is no noticeable jump between planets and satellites. The cumulative diagram “mass-radius” corresponds to Eq. (13) for quasars, stars, planets, and satellites, i.e. Eq. (13) describes the whole diagram.

In Fig. (6), the cumulative diagram “density-mass” is shown for quasars, stars, planets, and satellites of the solar

**Table 5. Comparison of calculated with Eqs. (13-15) values and observations for stars O5-M5, and for planets and satellites of the solar system.**

Object	$\log (r_{gr}/r)$	$\log m$ [g] Observed	$\log m$ [g] Eq. (13)	$\log \rho$ [g/cm <sup>3</sup> ] Observed	$\log \rho$ [g/cm <sup>3</sup> ] Eq. (14)	$\log r$ [cm] Observed	$\log r$ [cm] Eq. (15)
Stars O5	-4.921	35.079	34.898	-1.509	-2.061	11.989	11.894
Stars B0	-5.036	34.505	34.506	-1.252	-1.258	11.712	11.708
Stars B5	-5.119	34.146	34.145	-0.777	-0.789	11.434	11.429
Stars A0	-5.276	33.778	33.777	-0.513	-0.524	11.223	11.219
Stars A5	-5.301	33.602	33.602	-0.240	-0.247	11.073	11.070
Stars F0	-5.292	33.556	33.557	-0.122	-0.128	11.019	11.015
Stars F5	-5.337	33.477	33.482	-0.111	-0.105	10.989	10.987
Stars G0	-5.387	33.322	33.327	0.048	0.055	10.884	10.883
Stars G5	-5.367	33.265	33.269	0.223	0.229	10.806	10.805
Stars K0	-5.409	33.193	33.193	0.255	0.247	10.772	10.768
Stars K5	-5.387	33.140	33.143	0.418	0.419	10.700	10.698
Stars M0	-5.444	33.009	33.007	0.524	0.510	10.621	10.616
Stars M5	-5.495	32.602	32.609	1.158	1.171	10.274	10.274
Mercury	-9.6975	26.519	26.520	0.735	0.730	8.387	8.384
Venus	-8.9235	27.687	27.688	0.719	0.7155	8.782	8.779
Earth	-8.857	27.776	27.777	0.742	0.737	8.804	8.801
Mars	-9.551	26.807	26.809	0.594	0.593	8.530	8.527
Jupiter	-7.395	30.278	30.2795	0.124	0.119	9.8445	9.841
Saturn	-7.854	29.755	29.756	-0.161	-0.212	9.780	9.753
Uranus	-8.293	28.939	28.9395	0.104	0.104	9.4025	9.402
Neptune	-8.209	29.010	29.0115	0.215	0.213	9.390	9.388
Pluto	-11.076	25.116	25.117	0.301	-0.600	8.363	7.912
Moon	-10.2025	25.866	25.867	0.525	0.520	8.240	8.236
Io	-10.138	25.951	25.952	0.550	0.545	8.260	8.256
Europa	-10.341	25.681	25.682	0.479	0.475	8.193	8.190
Ganymede	-10.079	26.171	26.172	0.287	0.282	8.421	8.417
Callisto	-10.179	26.032	26.033	0.2645	0.260	8.382	8.378
Tethys	-11.766	23.792	23.7935	-0.018	-0.0225	7.729	7.726
Dione	-11.538	24.041	24.0425	0.169	0.164	7.750	7.747

Table 5. contd...

Object	$\log (r_g/r)$	$\log m$ [g] Observed	$\log m$ [g] Eq. (13)	$\log \rho$ [g/cm <sup>3</sup> ] Observed	$\log \rho$ [g/cm <sup>3</sup> ] Eq. (14)	$\log r$ [cm] Observed	$\log r$ [cm] Eq. (15)
Rhea	-11.3505	24.362	24.363	0.0895	0.085	7.883	7.880
Titan	-10.109	26.130	26.1315	0.276	0.271	8.411	8.4075
Iapetus	-11.440	24.255	24.256	0.034	0.030	7.866	7.863
Ariel	-11.460	24.131	24.132	0.221	0.217	7.763	7.759
Umbriel	-11.527	24.069	24.070	0.146	0.1415	7.767	7.764
Titania	-11.1785	24.547	24.5485	0.234	0.230	7.897	7.894
Oberon	-11.231	24.479	24.480	0.212	0.208	7.882	7.878
Triton	-10.629	25.331	25.332	0.315	0.311	8.131	8.128

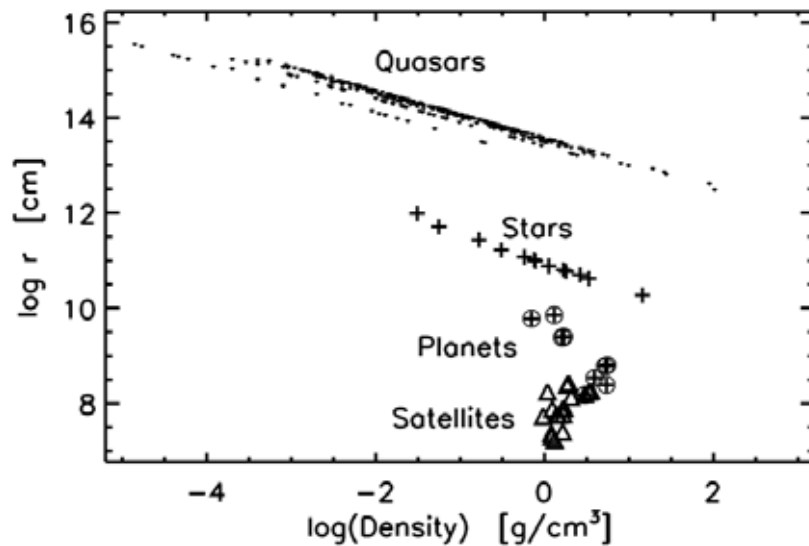


Fig. (7). Cumulative diagram of the “radius-density” relation for quasars (dots), stars (crosses), the 9 big planets of the solar system (encircled crosses), and for 19 satellites (triangles, the list is as in caption of Table 4).

system. The slopes of these diagrams are gradually decreasing and for satellites there is possibly no slope at all. As this slope concerns the changes of density, depending on mass, in the framework of the disintegration concept it could mean that the process (whatever it is) gets gradually less efficient, as it proceeds from quasars to satellites. This diagram corresponds to Eq. (14), which describes the whole diagram.

On Fig. (7), the cumulative diagram “radius-density” is also shown for quasars, stars, planets, and satellites of the solar system. Trends are clearly seen for QSOs, stars, and planets in the sense that larger dimensions correspond to smaller densities. In the framework of the disintegration concept this could mean that by the evolution with decreasing density dimensions increase, as it should be expected. This diagram is described by Eq. (15).

The similarity of respective diagrams for quasars, stars, planets and satellites raises the question, is it possible to construct a unified picture of the origin of structures of different

dimensions, based on the concept of disintegration of the original dense matter?

It is now being established that there are several relations – Eqs. (13-15), and the linear density relation (12) that hold for quasars, stars, planets and satellites. With that evidence, the conclusion seems inevitable that there has to be a link between these objects, possibly in their origin.

**7. DISCUSSION AND CONCLUDING REMARKS**

The average relations “mass-radius”, “density-mass”, and “radius-density” for quasars were established in [1-3]. The unusual fragmentation of these diagrams (Figs. 1-3) may have been perceived as a strange feature and remained so far unexplained. It is now being revealed as being possibly caused by the evolution of quasars and in agreement with the disintegration concept. Each one of the above relations is actually a family of relations, and each individual relation

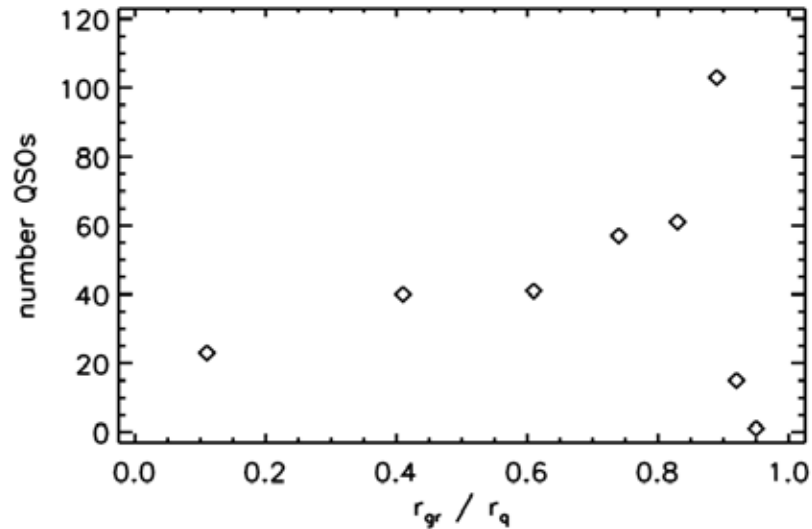


**Fig. (8).** Distribution of number of QSOs over  $r_{gr}/r_q$  for the sample of 341 QSOs.

from a family corresponds to a specific value of  $r_{gr}/r_q$ . By the evolution of quasars  $r_{gr}/r_q$  takes subsequently a series of discrete values, starting with 1. The last value in all series of relations is 0.11. Correspondingly, the respective diagram (“mass-radius”, or “density-mass”, or “radius-density”) also evolves, and a family of relations (parallel lines) is created, each individual relation having the same slope. That explains the fragmentation mentioned above. The small differences in coefficients between this study and the “average” treatment in [1-3] are due to the fragmentation and to the unequal “population” with QSOs of each individual relation (i.e. for each  $r_{gr}/r_q$  the number of QSOs is different, see Tables 1-3, and Fig. 8). The agreement of all family-relations (4, 9, and 11) with the observational data is undoubtedly an additional confirmation of consistency of the procedure, outlined in [1-3]. The evolution of the “mass-radius” relation may also reveal possible decrease of mass and increase of radius (Fig. 1). The evolution of the “density-mass” relation clearly shows the decrease of density (Fig. 2). The evolution of the “radius-density” relation shows increasing radius with decreasing density (Fig. 3).

The distribution of QSOs over  $r_{gr}/r_q$  is an interesting question in itself (Fig. 8). It shows a sharp maximum at 0.89 ( $z_{gr} = 1.96$ ), and a gradual decrease of number of QSOs to smaller values of  $r_{gr}/r_q$ . The interpretation of this distribution remains unexplained but two factors may be contributing to the distribution: the initial mass-distribution of QSOs, and the “specific-evolution-times” for a transition from one  $r_{gr}/r_q$  value to the next (smaller) one. As the initial mass-distribution of QSOs is unknown, it is not possible to reach conclusions about the “specific-evolution-times”. Yet, Fig. 8 leaves the impression of very fast evolution from  $r_{gr}/r_q = 1$  to  $r_{gr}/r_q = 0.89$ , and a sudden slow-down in evolution of quasars at  $r_{gr}/r_q = 0.89$ .

As shown in section 6, the Eqs. (13, 14, and 15), describing respectively the relations for quasars: “mass-radius”, “density-mass”, and “radius-density”, hold also for stars, planets, and satellites. This corroborates the suggestion that a unified concept of origin may be possible for different structures as quasars, stars, planets, and satellites.

The cumulative diagrams in (Figs. 5-7) show new features and raise additional questions:

- There are gaps (jumps) between the diagrams for different structures.
- The jumps decrease by the transition from quasars to planets.
- There is (possibly) no gap between the planets and the satellites.
- The trend of density over mass (Fig. 6) has a decreasing slope by the transition from quasars to planets, and for the satellites there may be no trend at all.

As density is an important mark in the disintegration concept, the decreasing density slope from quasars to planets may be an indication of gradual “exhaustion” of the process of disintegration by going to ever smaller structures.

If the concept of disintegration is correct, the jumps between diagrams for different structures may be due to the existence of different stages (successive cascades) of disintegration.

The applicability of a simple linear density relation (12) to different structures (in addition to relations (13-15)) is another indication in favor of unified concept of origin of different structures. All these common relations may be indicating to a link in the origin of the different structures: quasars, stars, planets, and satellites. The existence of such link could suggest that all these different structures may have a common “design” by their origin. Although this matter is far from clear, the evidence of common relations could present difficulties to the theory of gravitational collapse, now generally accepted. Indeed, how could it be possible for a random process of collapses on different scales (quasars, stars, planets, or satellites) to build all these structures following common relations? A random process is not expected to follow relations of this kind. It may be that a re-considering of origin of structures is necessary and the alternative could be the concept of disintegration, as suggested by Victor Ambartsumian ~60 years ago [31]. Specific models for such a concept are not yet possible and that is the problem.

**CONFLICT OF INTEREST**

The authors confirm that this article content has no conflicts of interest.

**ACKNOWLEDGEMENTS**

I am grateful to Dr D. Dimitrov for his valuable help in preparations of the figures.

**REFERENCES**

- [1] Panov KP. Study of possible local quasars I. The First Sample. *OAJ* 2011; 4: 14-26.
- [2] Panov KP, Dimitrov DP. Study of possible local quasars II: a sample of 225 QSOs. In: Thales, in Honor of Prof. Emeritus Michael E. Contadakis, 2013; pp. 78-105, ISBN 978-960-89704-1-0.
- [3] Panov KP. Study of possible local quasars and search for a quasar-stellar connection III: a sample of 341 QSOs. *OAJ* 2013; 6: 20-47.
- [4] Arp HC. Catalogue of discordant redshift associations. APEIRON. Montreal: Canada, 2003.
- [5] Arp HC. Quasars, Redshifts, and Controversies. *Interstellar Medium*. Berkley: USA, 1987.
- [6] Burbidge G. The reality of anomalous redshifts in the spectra of some QSOs and its implications. *Astron Astrophys* 1996; 309: 9-22.
- [7] Burbidge GR. Non-cosmological redshifts. *Publ Astron Soc Pac* 2001; 113: 899-902.
- [8] Hoyle F, Burbidge G. Anomalous redshifts in the spectra of extragalactic objects. *Astron Astrophys* 1996; 309: 335-44.
- [9] Burbidge G, Hewitt A, Narlikar JV, Gupta PD. Associations between quasi-stellar objects and galaxies. *Astrophys J Suppl Ser* 1990; 74: 675-730.
- [10] Williams LLR, Irwin M. Angular correlations between LBQS and APM: weak lensing by the large-scale structure. *Mon Not RAS* 1998; 298: 378-88.
- [11] Bell MB. Further evidence for large intrinsic redshifts. *Astrophys J* 2002; 566: 705-11.
- [12] Jain B, Scranton R, Sheth RK. Quasar-galaxy and galaxy-galaxy cross-correlations: model predictions with realistic galaxies. *Mon Not RAS* 2003; 345: 62-70.
- [13] Lopez-Corrodoira M, Gutierrez CM. Research on candidates for non-cosmological redshifts. In: Lerner EJ, Almeida JB, Eds. *AIP Conf Proc of First Crisis in Cosmology Conf*. NY, USA: 2006; 822: 75-92.
- [14] Burbidge G, Napier WM. Associations of high-redshift quasi-stellar objects with active, low-redshift spiral galaxies. *Astrophys J* 2009; 706: 657-64.
- [15] Burbidge EM, Burbidge GR, Solomon PM, Strittmatter PA. Apparent associations between bright galaxies and quasi-stellar objects. *Astrophys J* 1971; 170: 233-40.
- [16] Galianni P, Burbidge EM, Arp H, *et al*. The discovery of a high redshift x-ray emitting QSO very close to the nucleus of NGC 7319. *arXiv/astro-ph/0409215* 2004.
- [17] Carilli CL, van Gorkom JH, Stocke J. 3C232 and NGC 3067: Quasars, galaxies, and absorption lines. *Bull AAS* 1988; 20: 1027.
- [18] Carilli CL, van Gorkom JH, Stocke JT. Disturbed neutral hydrogen in the galaxy NGC 3067 pointing to the quasar 3C232. *Nature* 1989; 338: 134-6.
- [19] Arp H. A QSO 2.4 arcsec from a dwarf galaxy – the rest of the story. *Astron Astrophys* 1999; 341: L5-L8.
- [20] Gosset E, Moreau O, Surdej J, *et al*. Surveys of ultraviolet-excess quasar candidates in large fields. *Astron Astrophys Suppl Ser* 1997; 123: 529-68.
- [21] Arp H. X-ray observations of NGC 1097 and nearby quasars. *Astrophys Sp Sci* 1998; 262: 337-61.
- [22] Arp H, Burbidge EM, Chu Y, *et al*. NGC 3628: Ejection activity associated with quasars. *Astron Astrophys* 2002; 391: 833-40.
- [23] Arp H, Burbidge EM, Carosati D. Quasars and galaxy clusters paired across NGC 4410. *arXiv astro-ph/0605453* 2006.
- [24] Burbidge EM, Burbidge G. QSOs in the field of the seyfert galaxy NGC 5548. *Publ Astron Soc Pac* 2002; 114: 253-56.
- [25] Burbidge EM. Spectra of two quasars possibly ejected from NGC 4258. *Astron Astrophys* 1995; 298: L1-L4.
- [26] Burbidge EM. Spectra of two x-ray emitting quasi-stellar objects apparently ejected from the seyfert galaxy NGC 2639. *Astrophys J* 1997; 484: L99-L101.
- [27] Burbidge EM, Burbidge G. Ejection of matter and energy from NGC 4258. *Astrophys J* 1997; 477: L13-L15.
- [28] Arp H. Quasar creation and evolution into galaxies. *J Astrophys Astron* 1997; 18: 393-406.
- [29] Arp H, Burbidge EM, Chu Y, *et al*. NGC 3628: ejection activity associated with quasars. *Astron Astrophys* 2002; 391: 833-40.
- [30] Burbidge G. Two universes. *Astrophys Sp Sci* 1996; 244: 169-76.
- [31] Ambartsumian VA. La structure et l'évolution de l'univers. 11<sup>th</sup> Conseil de Physique Solvay 1958, Bruxelles.
- [32] Arp H. Quasar creation and evolution into galaxies. *J Astrophys Astron* 1997; 18: 393-406.
- [33] Arp H. Evolution of quasars into galaxies and its implications for the birth and evolution of matter. *APEIRON* 1998; 5: 135-42.

Received: January 30, 2014

Revised: June 22, 2014

Accepted: June 24, 2014

© Kiril P. Panov; Licensee *Bentham Open*.

This is an open access article licensed under the terms of the Creative Commons Attribution Non-Commercial License (<http://creativecommons.org/licenses/by-nc/3.0/>) which permits unrestricted, non-commercial use, distribution and reproduction in any medium, provided the work is properly cited.